CERN-ACC-2018-0035

Future Circular Collider

PUBLICATION

Initial Study of the Reconstruction of Boosted B-hadrons and τ-leptons at FCC-hh

Perez Codina, Estel () *et al.*

20 October 2018

The research leading to this document is part of the Future Circular Collider Study

The electronic version of this FCC Publication is available
on the CERN Document Server at the following URL :
<http://cds.cern.ch/record/2643897>

CERN-ACC-2018-0035

LCD-Note-2018-003
CERN-ACC-2018-0035
16 October 2018

Initial Study of the Reconstruction of Boosted B-hadrons and τ-leptons at FCC-hh

E. Perez[1)*], P. Roloff[*]

[*] *CERN, Switzerland*

Abstract

The FCC-hh project aims at studying proton-proton collisions at $\sqrt{s} = 100\,\text{TeV}$. In beyond the Standard Model scenarios, such high collision energy can produce unprecedented high-energy objects in the multi-TeV range. At high energies, particles like τ-leptons and B-hadrons are extremely boosted, since their masses are relatively small. Reconstructing the decay products of these boosted and long-lived particles is very challenging since the decay vertex can be very displaced and the decay products extremely collimated. This note addresses the challenge of reconstructing the tracks from all the charged daughter particles. For this purpose, events containing 3-prong τ-lepton decays and di-jet $b\bar{b}$ events are simulated. The distance between simulated hits produced by the decay daughters in a particular layer is used to provide a qualitative estimate of the tracking efficiency for boosted objects. The study is performed for various energies and detector granularities.

This work was carried out in the framework of the FCC Collaboration

[1] estel.perez.codina@cern.ch

1. Introduction

FCC-hh is a CERN-based future project to build a $\approx 100\,\text{km}$ long accelerator providing proton-proton collisions at $\sqrt{s} = 100\,\text{TeV}$. At such a collision energy, objects like τ-leptons and B-hadrons can be extremely boosted. For instance, in BSM benchmark scenarios like $Z' \to \tau^+\tau^-$ or $Z' \to t\bar{t}$, τ-leptons and b-jets can have momenta in the order of several TeV. In general, in order to reconstruct and identify the multi-prong signature of a long-lived particle such as a 3-prong τ-lepton decay or a B-hadron decay, the individual decay products need to be reconstructed. For such boosted objects, reconstructing the decay products is challenging since their production vertex can be very displaced from the interaction point and because the decay products can be very collimated.

The minimum number of hits required to reconstruct a track defines a displaced vertex reconstruction "acceptance", i.e. a limit on the flight distance of the mother particle. For the FCC-hh detector it has been found that eight hits per track are required to keep the fake rate at a reasonable level [1]. Therefore, only the decay products of particles decaying before the 8^{th} outermost layer traverse enough layers to be reconstructed. Figure 1 illustrates these long-lived particle decays in FCC-hh. This acceptance has a

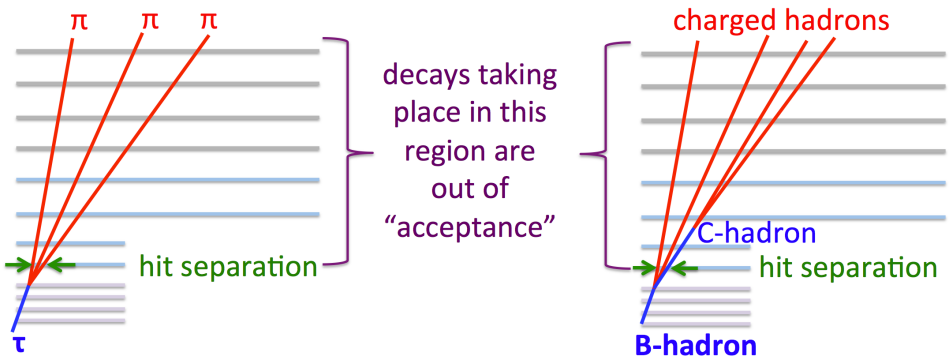

Figure 1: Illustrative sketch of a 3-prong τ-lepton and a B-hadron decaying inside the FCC-hh tracker.

direct impact on the maximum tagging performance achievable through secondary vertex identification for a given τ-lepton/B-hadron energy. The impact of this effect is less important in the forward region, since the tracker is one order of magnitude longer in the Z direction than in R and has a larger number of detection layers.

In addition to producing hits in at least the eight outermost layers, all the eight hits need to be unambiguously associated to that track. Hence, the hits must be separated enough in all layers to produce distinguishable clusters. In this study, the efficiency to reconstruct the tracks of all the decay products is estimated by evaluating the distance between hits from close-by tracks in a particular detector layer. This efficiency is calculated as a function of the single point resolution and for different τ and b-jet energies. For this purpose, events containing 3-prong τ-lepton decays as well as $b\bar{b}$ events are generated and fully simulated. This study uses simulated hits, while the effect of detector granularity is estimated *ad hoc*. The impact of pile-up interactions is not considered. It is expected that at high boost the decay products are closer to another particle from the same decay than to particles from pile-up interactions [2].

This document is structured as follows. Section 2 describes the Monte Carlo samples, detector geometry and software used in this study. Section 3 introduces the concept of "hit separation efficiency", and in Section 4 the results for τ and B-hadron decays are presented. The conclusions and outlook are summarised in Section 5.

2. Simulation

2.1. 3-prong τ-lepton samples

Monte Carlo (MC) samples of di-τ events at various energies are generated using Whizard 1.95 [3]. Fragmentation and hadronisation are modelled using Pythia6 [4]. No Initial State Radiation (ISR) or pile-up interactions are included in the simulation. The τ decays are simulated within the TAUOLA [5][6] package. The τ-leptons are produced back-to-back and very centrally, with a pseudorapidity of $|\eta| < 0.175$. Seven samples with different τ energies are produced :

- "E(τ) = 100 GeV"
- "E(τ) = 200 GeV"
- "E(τ) = 500 GeV"
- "E(τ) = 1000 GeV"
- "E(τ) = 2000 GeV"
- "E(τ) = 5000 GeV"
- "E(τ) = 10 000 GeV"

Events with at least three charged pions are selected. This effectively requires that the event has at least one of the τ-leptons decaying hadronically to three charged pions.

2.2. B-jet samples

Another set of MC samples with $b\bar{b}$ di-jet events in p-p collisions at $\sqrt{s} = 100$ TeV is generated using Madgraph5 [7]. The b-quarks are produced very centrally, with a pseudorapidity of $|\eta| < 0.05$, and with a transverse momentum (p_T) within a narrow range. Seven samples with different p_T ranges are produced:

- "$p_T = 50$ GeV" : 47.5 GeV $< p_T(b) <$ 52.2 GeV,
- "$p_T = 100$ GeV" : 95 GeV $< p_T(b) <$ 105 GeV,
- "$p_T = 200$ GeV" : 195 GeV $< p_T(b) <$ 205 GeV,
- "$p_T = 500$ GeV" : 490 GeV $< p_T(b) <$ 510 GeV,
- "$p_T = 1000$ GeV" : 990 GeV $< p_T(b) <$ 1010 GeV,
- "$p_T = 2000$ GeV" : 1950 GeV $< p_T(b) <$ 2050 GeV,
- "$p_T = 5000$ GeV" : 4950 GeV $< p_T(b) <$ 5050 GeV.

The events include both ISR and Final State Radiation (FSR). Fragmentation and hadronisation are modelled using Pythia6 [4]. As a result, the generated quark p_T distribution is smeared with respect to the ranges listed above [2]. The MC simulation does not include multiple interactions or pile-up events.

[2] The quark p_T before ISR and FSR is sometimes referred to as "jet p_T" in this document, to refer to the samples described above.

2.3. Detector geometry and software

The FCC-hh tracker geometry version v3.03 [8] in its flat (non-tilted) configuration is used as reference to perform this study. In the barrel region, the FCC-hh detector consists of four pixel layers with average radii of 25 mm, 60 mm, 100 mm and 150 mm respectively, as depicted in Figures 2 and 3. The material budget is $X/X_0 = 1\%$ per layer, which includes an estimation for the non-sensitive material like cables and support structures. Surrounding the vertex layers, there are four layers of macro-pixels, with radii of 270 mm, 400 mm, 530 mm and 742 mm and a material budget of $X/X_0 = 2\%$ per layer. Finally, in the outermost part of the tracker there are four striplet layers with radii of 0.9 m, 1.1 m, 1.3 m and 1.5 m, respectively, and $X/X_0 = 2.5\%$ of material budget per layer. The sensor pitch in $R-\varphi$ and Z is $25 \times 50\,\mu m^2$, $33 \times 400\,\mu m^2$ and $33\,\mu m \times 50\,mm$ for pixels, macropixels and striplets, respectively. The tracker is immersed in a 4 T solenoidal magnetic field. The barrel tracker geometry, granularity and material budget are summarised in Table 1.

Barrel Layer	**layer Radius [mm]**	**Material budget** X/X_0	$R-\varphi$ **granularity** [μm]	Z **granularity** [μm]
1	25	1%	25	50
2	60			
3	100			
4	150			
5	270	2%	33	400
6	400			
7	530			
8	742			
9	937	2.5%	33	50000
10	1132			
11	1327			
12	1540			

Table 1: FCC-hh tracker geometry, granularity and material budget.

The tracker geometry is defined using tkLayout [9] and translated to the DD4hep [10] format. The particle interactions with the detector are simulated using DDSim [11], which is based on GEANT4 [12–14]. The simulated hits are not digitised.

2.4. Properties of τ-lepton and B-hadron decays in the FCC-hh detector

This section describes briefly the kinematic properties of 3-prong τ-lepton and B-hadron decays in the FCC-hh detector. Figure 4 shows the τ-lepton decay vertex position in the radial direction for the different energy values. Figure 5 presents the corresponding τ-lepton p_T spectra. Figures 6 and 7 show the corresponding quantities for B-hadrons.

Table 2 shows the fraction of τ-leptons that decay before each of the detector layers for various E(τ) samples. For the E(τ) = 5 TeV sample more than half of the τ-leptons decay after the 4^{th} detection layer.

Table 3 shows the fraction of B-hadrons that decay before each of the detector layers, for various p_T samples. The denominator includes only B-hadrons that have a non-zero flight distance, including decays happening beyond the last tracker layer. In the $p_T = 5$ TeV sample, more than half of the B-hadrons decay after the 3^{rd} detection layer.

About 71% of central B-hadrons in a p_T(b) = 5 TeV jet and 68% of central τ-leptons with E(τ) = 5 TeV decay before the 8^{th} outermost layer. For those B-hadrons and τ-leptons which decay after that layer, the decays are out of acceptance and their secondary vertex and daughter tracks cannot be reconstructed.

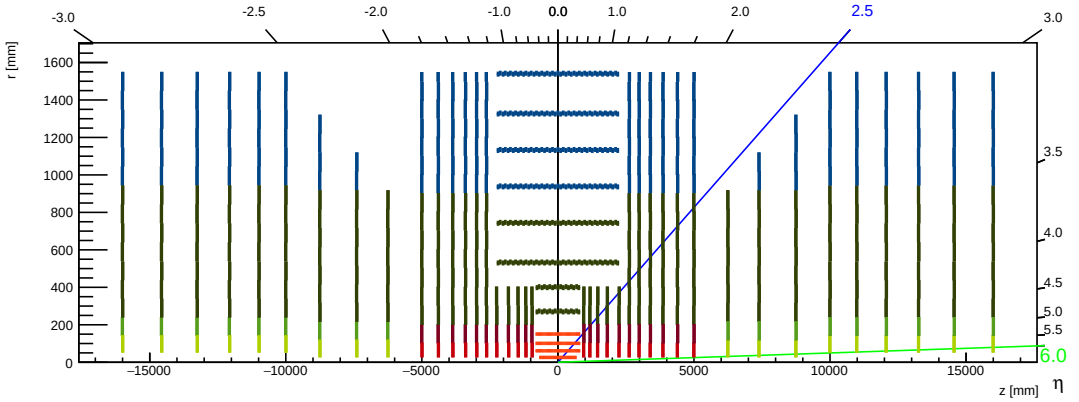

Figure 2: FCC-hh tracker. The different colours indicate different sensor granularities.

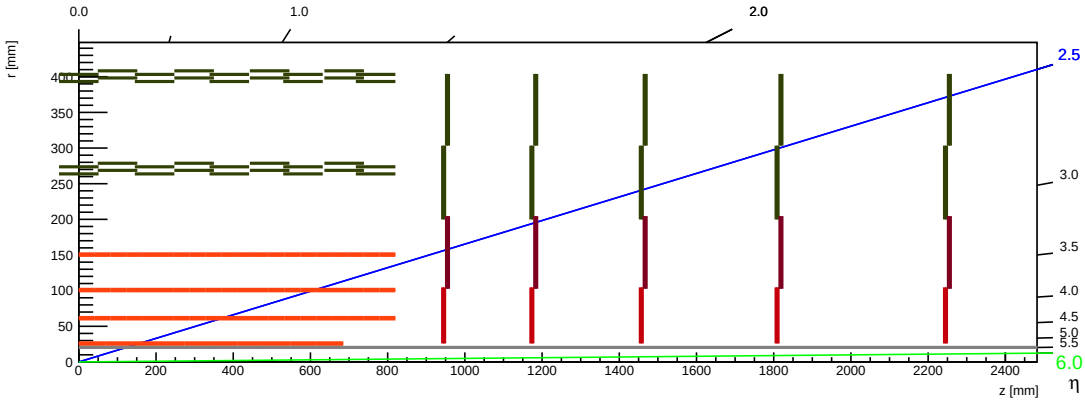

Figure 3: Inner part of the FCC-hh tracker. The different colours indicate different sensor granularities.

Layer	layer R[mm]	E(τ)[GeV] =	100	200	500	1000	2000	5000	10000
Beampipe	20		0.99	0.89	0.58	0.36	0.20	0.09	0.04
1	25		1.00	0.94	0.67	0.44	0.25	0.11	0.06
2	60		1.00	1.00	0.93	0.73	0.48	0.24	0.12
3	100		1.00	1.00	0.99	0.88	0.65	0.35	0.20
4	150		1.00	1.00	1.00	0.96	0.80	0.48	0.28
5	270		1.00	1.00	1.00	1.00	0.94	0.68	0.44
6	400		1.00	1.00	1.00	1.00	0.98	0.81	0.57
7	530		1.00	1.00	1.00	1.00	1.00	0.89	0.67
8	742		1.00	1.00	1.00	1.00	1.00	0.95	0.79
9	937		1.00	1.00	1.00	1.00	1.00	0.98	0.86
10	1132		1.00	1.00	1.00	1.00	1.00	0.99	0.91
11	1327		1.00	1.00	1.00	1.00	1.00	1.00	0.94
12	1540		1.00	1.00	1.00	1.00	1.00	1.00	0.96

Table 2: Fraction of τ-leptons decaying before each detector layer for the different E(τ) samples.

3. Hit separation efficiency

In this study, it is assumed that to reconstruct a 3-prong τ-lepton or a B-hadron decay, all the decay products need to be reconstructed. In order to reconstruct the tracks from all decay products, the daughter particles need to traverse at least the eight outermost layers. In addition to producing hits in the eight outermost layers, all eight hits need to be unambiguously associated to the particle's track. Hence, the

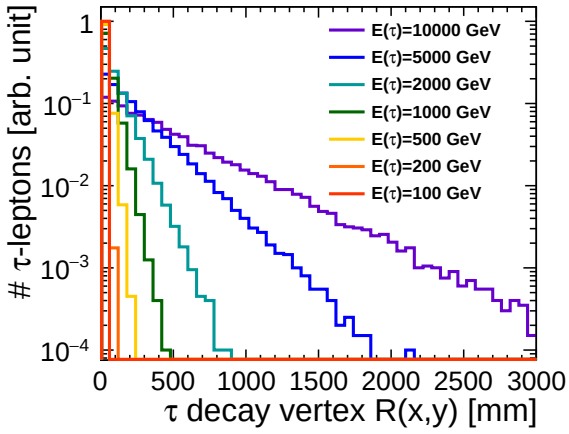

Figure 4: τ-lepton decay vertex position in the radial direction in central $\tau^+\tau^-$ events for various τ energies.

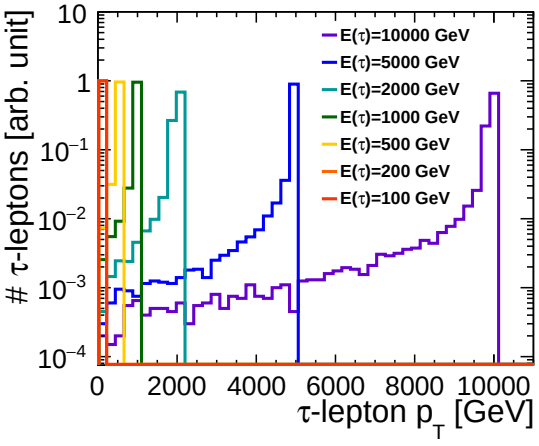

Figure 5: τ-lepton p_{T} distribution in central $\tau^+\tau^-$ events for various τ energies.

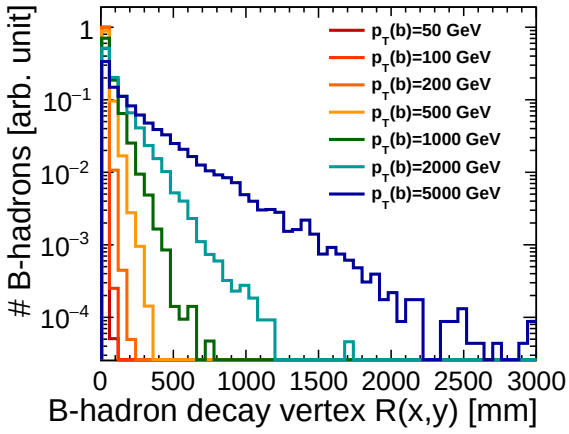

Figure 6: B-hadron decay vertex position in the radial direction for different b-quark p_{T} values.

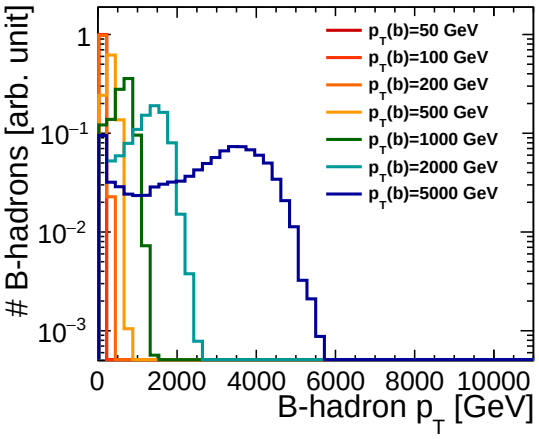

Figure 7: B-hadron p_{T} distribution for different b-quark p_{T} values.

hits from different particles must be sufficiently separated to produce distinguishable clusters in all layers. In this study, it is assumed that if the distance between two hits in a given layer is larger than twice the sensor pitch in either the R-φ or the Z direction, the hits will form separate clusters. For each event the closest pair of hits in a particular layer is selected, and their separation in the R-φ and in the Z directions is calculated. Since the closest pair of hits is calculated per event, in events where the two τ-leptons decay into three prongs, only the decay with the closest hits is considered. Therefore this "per-event" efficiency is a conservative estimate of the efficiency "per-decay". In the case of $\mathrm{b\bar{b}}$ events, the same applies for B-hadron decays. In addition, the B-hadron decay chain can include more than one decay vertex. If a first decay vertex happens before the considered layer but a second subsequent decay happens afterwards, the efficiency will take into account only the hits from stable particles generated in the first secondary vertex. Assuming that to identify a b-jet it is sufficient to reconstruct one of its secondary vertices, this efficiency will be related to the capability to tag both b-jets in the event.

The "hit separation efficiency" is defined as the fraction of closest pairs of hits, which form separated

Layer	layer R[mm]	p_T (b)[GeV]=	50	100	200	500	1000	2000	5000
Beampipe	20		1.00	0.96	0.83	0.58	0.40	0.28	0.19
1	25		1.00	0.98	0.89	0.66	0.46	0.32	0.22
2	60		1.00	1.00	0.99	0.89	0.72	0.53	0.34
3	100		1.00	1.00	1.00	0.97	0.86	0.67	0.44
4	150		1.00	1.00	1.00	0.99	0.94	0.79	0.55
5	270		1.00	1.00	1.00	1.00	0.99	0.92	0.71
6	400		1.00	1.00	1.00	1.00	1.00	0.97	0.82
7	530		1.00	1.00	1.00	1.00	1.00	0.99	0.88
8	742		1.00	1.00	1.00	1.00	1.00	1.00	0.94
9	937		1.00	1.00	1.00	1.00	1.00	1.00	0.97
10	1132		1.00	1.00	1.00	1.00	1.00	1.00	0.98
11	1327		1.00	1.00	1.00	1.00	1.00	1.00	0.99
12	1540		1.00	1.00	1.00	1.00	1.00	1.00	0.99

Table 3: Fraction of B-hadrons decaying before each detector layer for the different p_T samples.

clusters in the 8th outermost layer. It is assumed that if the two particles can be separated on that layer, they can also be separated in the subsequent outer layers. This is because the granularity in R-φ is the same in the eight outermost layers and, as shown later in this document, in the default tracker design the R-φ granularity drives the hit separation efficiency. This efficiency is calculated as a function of the single point resolution and for different b-jet and τ-lepton energies. Digital readout is assumed throughout the tracker and therefore the single point resolution (σ) is estimated from the detector pitch as: $\sigma = \text{pitch}/\sqrt{12}$.

4. Results

4.1. τ-lepton decays

Figure 8 shows the hit separation efficiency versus R-φ and Z single point resolutions for 3-prong decays of τ-leptons of various energies. The 8th outermost layer has a default single point resolution of $9.5 \times 115\,\mu\text{m}^2$. To understand the effect of different granularities, the variations of the R-φ single point resolution are performed while keeping the Z single point resolution at its default value, and vice-versa.

For $\text{E}(\tau) \leq 200\,\text{GeV}$ the hit separation efficiency is close to 100%. For high-energy τ-leptons of $\text{E}(\tau) > 1\,\text{TeV}$, the efficiency drops rapidly with increasing single point resolution. The efficiency has a stronger dependence on the resolution in R-φ than in Z. This is because the sensors of the considered layer have a more than ten times larger pitch in the Z direction than in the R-φ direction. Therefore, it is more likely that the hits are separated in the R-φ direction. In 36% of the events with 3-prong decays of τ-leptons of $\text{E}(\tau) = 5\,\text{TeV}$ it will be possible to reconstruct all the daughter tracks with the current detector granularity. The percentage may increase to over 60% if the single point resolution in R-φ direction is halved.

4.2. B-hadron decays

Figure 9 shows the hit separation efficiency for B-hadron decays. Only the stable particles from a B-hadron decay chain are considered. Therefore, the hits produced by charged B- and C-hadrons are not taken into consideration in the calculations.

The hit separation efficiency decreases with jet p_T and single point resolution. For $p_T(\text{b}) > 1\,\text{TeV}$, a significant fraction of B- and C-hadrons reach the 8th outermost layer undecayed. The undecayed B-

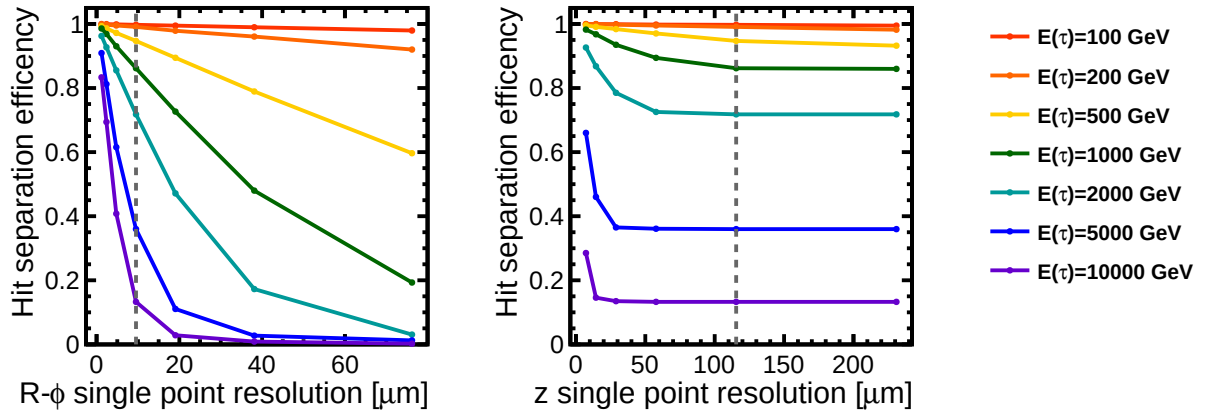

Figure 8: Hit separation efficiency in central $\tau^+\tau^-$ events for various τ energies versus the R-φ (left) and Z (right) single point resolution. The vertical lines illustrate the default sensor single point resolution in the 8$^{\text{th}}$ outermost layer.

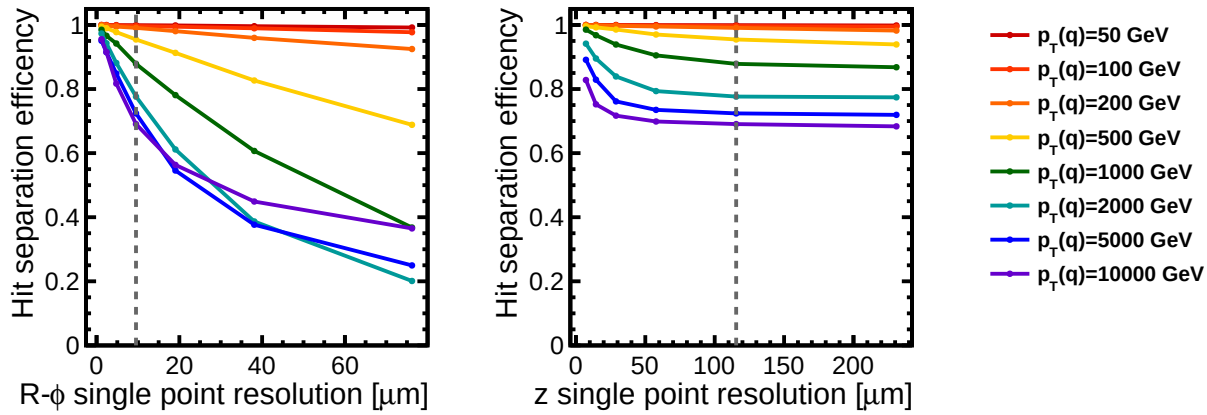

Figure 9: Hit efficiency for $b\bar{b}$ sample versus the R-φ (left) and Z (right) single point resolution. The vertical lines illustrate the default sensor single point resolution in the 8$^{\text{th}}$ outermost layer.

hadrons do not enter the efficiency calculation, and the undecayed C-hadrons do not enter the "closest hit pair" calculation. Thus the estimated efficiency may appear to be larger than for lower-p_{T} jets. For B-hadrons in jets of $p_{\text{T}} = 5\,\text{TeV}$ the probability that all the decay products are reconstructed is 72%, and may increase to 85% if the single point resolution in the R-φ direction is be halved.

5. Conclusions

This study shows how the capability to reconstruct all the decay products of a long-lived particle decay rapidly decreases with increasing boost. This is partially due to the secondary vertex acceptance, which depends on the overall size of the tracker and number of layers. However, it is also caused by the hit separation performance, which depends on the detector granularity. It is found that even a small improvement in the R-φ granularity would provide a significant gain in the identification of the extremely boosted objects.

6. Outlook

This section briefly describes next steps and possible further studies.

Calculate per-object efficiency The hit separation efficiency is calculated per event, i.e., the closest pair of hits in the event is considered. This implies that, for events where both τ-leptons decay to 3 prongs and in the $b\bar{b}$ events, the most collimated of the two objects is selected. Therefore the hit separation efficiency, as calculated in this document, underestimates the efficiency for a single object to have all its daughters reconstructed.

Consider distance to all hits In this document, only the hits from stable daughter particles are considered. As explained in the text, in the case of B-hadrons this causes an overestimation of the efficiency at high p_T since the B-hadron and C-hadron hits are not considered. One could, on one side, repeat the study by considering all the particles involved in the decay (even if unstable). On the other side, one could consider also the particles in the event that are not involved in the B-hadron decay. The latter is expected to have a negligible effect at high p_T, but could potentially have a visible effect at lower energies.

Consider hits from pile-up events In line with the discussion above, one could simulate the pile-up events and consider the hits from those particles in the closest-hit calculation. As before, the effect is expected to be largest at lower p_T. It would be interesting to estimate at which jet p_T the effect of pile-up hits dominates over the effect of boosted decays, i.e., how often the closest hit is from the boosted object decay, and how often from a pile-up particle.

A. Hit separation efficiency: examples

The hit separation efficiency is based on the distance between the closest hit pair. Only hits from stable particles are considered in the calculation of the closest hit pair. The hits created by the charged unstable particles (B-harons and C-hadrons) are not taken into account. Depending on where the B- and C-hadron decay, there are three possible cases, illustrated and explained in Figure 10.

References

[1] E. Perez Codina, P. G. Roloff, *Tracking and Flavour Tagging at FCC-hh*, tech. rep. CERN-ACC-2018-0027, Geneva: CERN, 2018, URL: https://cds.cern.ch/record/2635893.

[2] E. Perez Codina, P. G. Roloff, *Hit multiplicity approach to b-tagging in FCC-hh*, tech. rep. CERN-ACC-2018-0023, Geneva: CERN, 2018, URL: https://cds.cern.ch/record/2631478.

[3] W. Kilian, T. Ohl, J. Reuter, *WHIZARD: Simulating Multi-Particle Processes at LHC and ILC*, Eur. Phys. J. **C71** (2011) 1742, DOI: 10.1140/epjc/s10052-011-1742-y, arXiv: 0708.4233 [hep-ph].

[4] T. Sjostrand, S. Mrenna, P. Z. Skands, *PYTHIA 6.4 Physics and Manual*, JHEP **05** (2006) 026, DOI: 10.1088/1126-6708/2006/05/026, arXiv: hep-ph/0603175 [hep-ph].

[5] S. Jadach, J. H. Kuhn, Z. Was, *TAUOLA: A Library of Monte Carlo programs to simulate decays of polarized tau leptons*, Comput. Phys. Commun. **64** (1990) 275, DOI: 10.1016/0010-4655(91)90038-M.

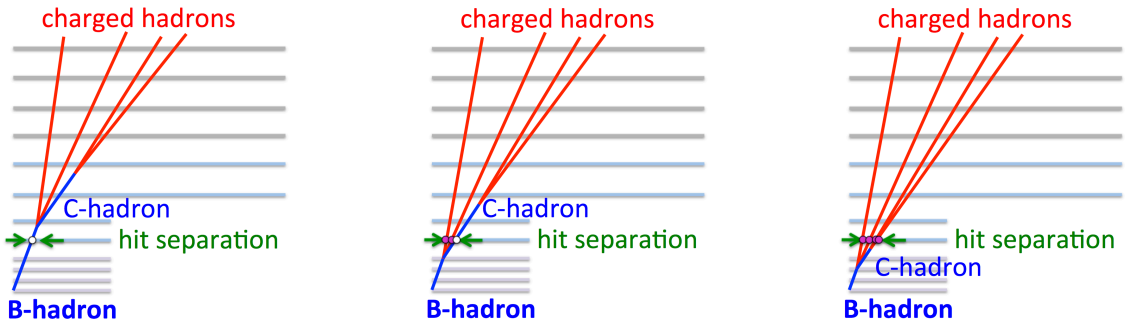

(a) Case A: B-hadron decays after the considered layer. The only hit in the layer is that of the B-hadron (in white). Since the B-hadron is not stable, the hit is not considered. No hits from this jet are considered, therefore the jet is effectively not considered.

(b) Case B: B-hadron decays before the considered layer, but the C-hadron decays after it. The hit from the C-hadron (in white) is not considered because the C-hadron is not stable. The hits from the other stable daughters of the B-hadron (in magenta) are considered.

(c) Case C: Both the B- and C-hadron decay before the considered layer. All the hits from the stable daughters (in magenta) are considered.

Figure 10: Hits considered in the calculation of the closest hit pair. Illustration of the three possible cases concerning the flight distance of unstable hadrons in the B-hadron decay chain.

[6] N. Davidson et al., *Universal Interface of TAUOLA Technical and Physics Documentation*, Comput. Phys. Commun. **183** (2012) 821, DOI: 10.1016/j.cpc.2011.12.009, arXiv: 1002.0543 [hep-ph].

[7] J. Alwall et al., *The automated computation of tree-level and next-to-leading order differential cross sections, and their matching to parton shower simulations*, JHEP **07** (2014) 079, DOI: 10.1007/JHEP07(2014)079, arXiv: 1405.0301 [hep-ph].

[8] *FCC-hh Layout v3.03*, URL: http://fcc-tklayout.web.cern.ch/fcc-tklayout/FCChh_v3.03/index.html.

[9] G. Bianchi, CMS, *tkLayout: a design tool for innovative silicon tracking detectors*, JINST **9** (2014) C03054, DOI: 10.1088/1748-0221/9/03/C03054.

[10] M. Frank et al., *DD4hep: A Detector Description Toolkit for High Energy Physics Experiments*, J. Phys. Conf. Ser. **513** (2014) 022010, DOI: 10.1088/1742-6596/513/2/022010.

[11] M. Petrič et al., *Detector simulations with DD4hep*, J. Phys. Conf. Ser. **898** (2017) 042015, DOI: 10.1088/1742-6596/898/4/042015.

[12] S. Agostinelli et al., *Geant4 - a simulation toolkit*, Nuclear Instruments and Methods in Physics Research Section A: Accelerators, Spectrometers, Detectors and Associated Equipment **506** (2003) 250, ISSN: 0168-9002, DOI: https://doi.org/10.1016/S0168-9002(03)01368-8, URL: http://www.sciencedirect.com/science/article/pii/S0168900203013688.

[13] J. Allison et al., *Geant4 developments and applications*, IEEE Transactions on Nuclear Science **53** (2006) 270, ISSN: 0018-9499, DOI: 10.1109/TNS.2006.869826.

[14] J. Allison et al., *Recent developments in Geant4*,
Nuclear Instruments and Methods in Physics Research Section A: Accelerators, Spectrometers, Detectors and Associated Equipment **835** (2016) 186, ISSN: 0168-9002,
DOI: https://doi.org/10.1016/j.nima.2016.06.125, URL: http://www.sciencedirect.com/science/article/pii/S0168900216306957.